

Review

Facet-controlled assembly for organizing metal-organic framework particles into extended structures

Zhongwu Ren,^{1,3} Nannan Zhang,^{1,3} Yuanyuan Wu,¹ Xue Ding,² Xiaoxin Yang,¹ Yuhan Kong,¹ and Hang Xing^{1,*}

SUMMARY

Metal-organic frameworks (MOFs) are crystalline porous materials characterized by their high porosity and chemical tailorability. To realize the full potential of synthesized MOFs, it is important to transform them from crystalline solid powders into materials with integrated morphologies and properties. One promising approach is facet-controlled assembly, which involves arranging individual crystalline MOF particles into ordered macroscale structures by carefully controlling the interactions between particles. The resulting assembled MOF structures maintain the characteristics of individual particles while also exhibiting improved properties overall. In this article, we emphasize the essential concepts of MOF assembly, highlighting the impact of building blocks, surface interactions, and Gibbs free energy on the assembly process. We systematically examine three methods of guiding facet-controlled MOF assembly, including spontaneous assembly, assembly guided by external forces, and assembly through surface modifications. Lastly, we offer outlooks on future advancements in the fabrication of MOF-based material and potential application exploration.

BACKGROUND

Metal-organic frameworks (MOFs) are a type of two-dimensional (2D) or three-dimensional (3D) crystalline coordination polymers formed by linking metal ions or metal-containing clusters with multivalent organic ligands via coordination interactions.^{1,2} Because MOF materials feature long-range extended modular framework structures, they possess distinctive characteristics. They are generally highly porous and chemically tunable, making them useful for adsorption, gas separation, catalysis, and biomedical applications.^{3–5} Because purified MOFs are usually obtained as crystalline solid powders, it is necessary to transform these individual loose pieces into macroscopic functional materials with integrated morphologies and properties to fully realize the potential of MOF materials in practical uses, particularly for industry applications.^{6,7}

To date, various fabrication techniques have been developed for the manufacturing of MOFs, transforming them from powders into solid forms. Notable methods include direct processing, monolithic growth, and mixed-matrix membrane (MMM).^{8–10} Direct processing methods, such as pressing and hot-pressing, are quite efficient and straightforward ways to form dense, uniform, and shape-controllable macroscopic MOF-based materials.^{11,12} However, it has been reported that during the processing, the crystal framework and intrinsic porosity may be imparted, negatively affecting the performance. The formation of monolithic matters can produce a macroscopic film or bulk MOF material with high stability, few defects, and controllable dimensions and orientations. However, the pores and open channels may be blocked during the growth process.¹³ A common approach to using MOF for practical separation applications is to mix MOF powders with polymer matrixes to create MMMs. With this approach, it is possible to create large, self-supporting materials that are strong, flexible, and with improved separation performance.^{14,15} However, MOFs have a relatively low mass content in an MMM, and the exposed metal centers and accessible voids might be compromised, resulting in reduced adsorption capacity.^{7,9,14} Despite the achievements of using the previously mentioned approaches for the fabrication of MOF-based macroscopic functional materials, the materials generated are normally polycrystalline containing randomly organized MOF particles with overall isotropic physiochemical properties. The lack of control in the orientation and long-range order might lead to low mass transfer efficiency and decreased catalytic activities. Therefore, the development of methods that can produce MOF-based macroscopic materials possessing long-range ordered structures and well-preserved anisotropic properties is in great need.^{16–18}

To overcome this challenge, a promising strategy involves the implementation of programmable assembly or self-assembly methods. Different from the approaches mentioned previously, the self-assembly approach directly employs physical and chemical interactions at particle-particle interfaces to guide the formation of macroscopic materials from individual building blocks, which leads to higher MOF content

¹Institute of Chemical Biology and Nanomedicine, State Key Laboratory of Chemo/Biosensing and Chemometrics, Hunan Provincial Key Laboratory of Biomacromolecular Chemical Biology, School of Chemistry and Chemical Engineering, Hunan University, Changsha, Hunan 410082, China

²School of Design and Art, Hunan University, Changsha, Hunan 410082, China

³These authors contributed equally

*Correspondence: hangxing@hnu.edu.cn

<https://doi.org/10.1016/j.isci.2023.107867>



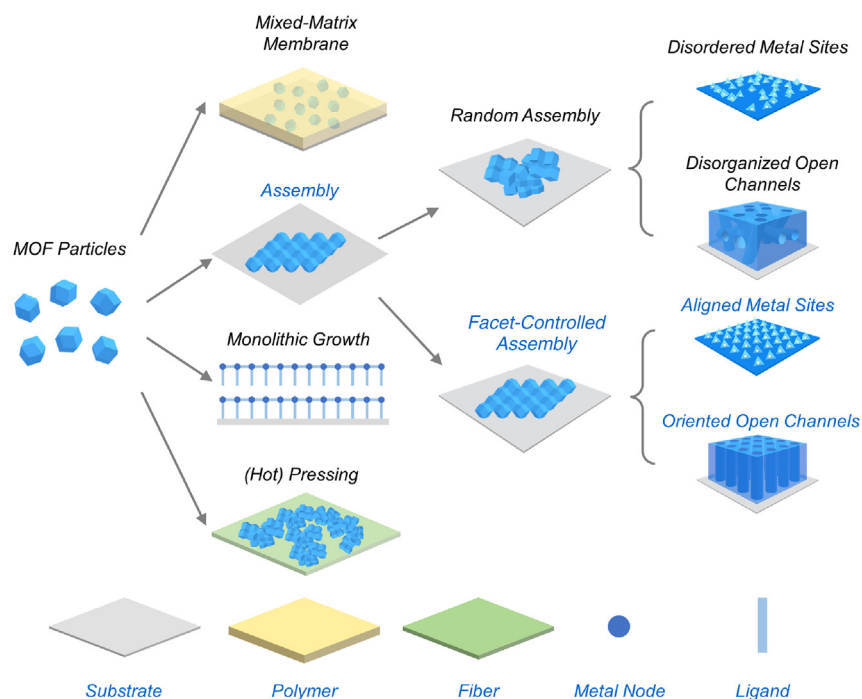


Figure 1. Comparison of facet-controlled assembly with other MOF processing approaches

The facet-controlled assembly of MOF particles results in well-aligned metal sites and oriented open channels in the assembled structure.

and better controllability. These approaches can effectively organize individual MOF particles into extended, highly ordered structures.^{1,6,8,19} Cohen et al. modified MOF particles with polymers and achieved self-supporting MOF films with a MOF content exceeding 85% through gas-liquid interface self-assembly.¹⁶ More importantly, a major advantage of the MOF assembly approach is that it permits a high degree of control over the facets and organizations during the assembly process, thereby generating macroscopic MOF particle arrays and even superlattices that can have long-range ordered structures.^{20,21} As each MOF building block represents a small particle, ordered MOF assemblies can be regarded as a macroscopic amplification of the microscopic crystal. Compared with other MOF processing approaches including MMM, monolithic growth, and hot-pressing, the assembled MOF material can inherit the anisotropic and facet-selective structural properties associated with crystal lattices, including well-aligned metal sites and oriented open channels, leading to enhanced efficiency and selectivity of mass transportation and other physical properties (Figure 1).^{22–25} As an example, the Cu-MOF films with aligned (001) orientation exhibited significantly enhanced electric and photocurrent properties in comparison to the Cu-MOF films with (100) orientation.²⁶ Moreover, the assembly of MOF particles in a well-controlled orientation was reported to enhance the mass transfer efficiency and gas permeability of the membrane.²⁷ By comparison, when MOF particles are arranged randomly, the arrangement of metal sites and pores is also disordered, thereby limiting their usage in applications involving catalysis and mass transfer.

Here, in this article, we discuss how facet-controlled self-assembly of MOF particles can be used to generate long-range ordered functional materials, aiming to provide a new perspective on producing functional MOF materials for practical use (Figure 2). During our preparation of this perspective, we became aware of Daniel Maspoch et al.'s recent review on the self-assembly of MOF particles, which shares some conceptual similarities with our work.²⁸ Our perspective article focuses on highlighting the distinctive features of single-crystalline MOF particles with precisely controlled morphologies and crystal habits. This control enables facet-guided interactions, leading to the formation of extended and highly ordered structures, including superlattices. This perspective article comprises the following sections. Firstly, we discuss some fundamental concepts in MOF assembly, highlighting the unique properties of the crystalline building blocks, the tailorable inter-particle interactions, and the thermodynamic understanding of the self-assembly process. After that, we systematically review the reports on facet-controlled self-assembly of MOFs from the viewpoint of the forces that govern the interaction, including spontaneous assembly, external force-guided assembly, and surface modification-induced assembly. Lastly, we provide perspective and outlook on how current MOF assembly strategies can be improved in terms of efficiency and structural control. The potential application of these ordered MOF assemblies in different scenarios has also been discussed.

BASIC CONCEPTS OF MOF ASSEMBLY

Programmable assembly or self-assembly refers to the deliberate control of the organization process, where building blocks come together to form ordered structures or specific patterns, either with or without the use of external stimuli. George M. Whitesides introduced the term “self-assembly” in the 1980s to describe the spontaneous arrangement process of building blocks at various scales.^{29–32} In 1996, Chad A. Mirkin

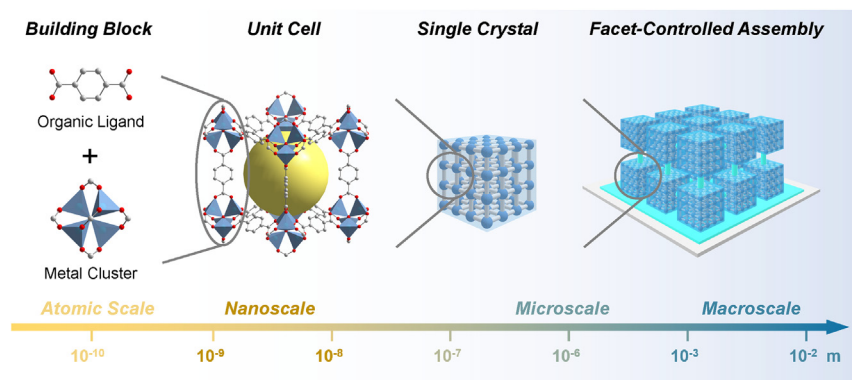


Figure 2. Scheme showing the facet-controlled assembly process to generate functional MOF materials in different scales, from molecular building blocks to crystalline particles, then to the macroscopic ordered particle arrays

and Paul Alivisatos applied the concept of “programmable assembly” to control the organization of gold nanoparticles using surface-modified DNA strands through sequence programmable Watson-Crick base-pairing interactions.^{33,34} Over the past decades, various materials, such as DNA, proteins, quantum dots, polystyrene particles, and live mammalian cells, have been organized into long-range ordered arrangements through diverse assembly processes.^{35–39} Similarly, MOF particles, acting as crystalline building blocks, adhere to the same principle and have been shown to form assembled structures at micro- to macroscales. This section presents some basic concepts of MOF assembly.

Utilizing single-crystalline MOF particles as functional building blocks

Like other crystalline materials, MOF is constructed from repeating units containing multivalent metal clusters and organic ligands and normally generates single-crystal particles with well-defined crystal habits. Depending on the symmetry and organization of ligands and metals used in different MOFs, the underlying lattices as well as the crystal habits vary dramatically. For example, MOF-5 and UiO-66, two iconic MOF constructs using BDC as ligands, both belong to cubic lattices with the former one simple cubic and the latter one face-centered cubic. However, due to the differences in symmetry and connectivity between the Zn₄ and Zr₆ clusters, these two MOFs tend to grow along different crystal planes, resulting in particles exposing different facets. MOF-5 tends to grow along the (111) plane and expose the (100) facet, forming particles with cubic shapes, while UiO-66 tends to grow along the (100) plane and expose the (111) plane, forming particles with octahedral shapes.^{40,41} In Table 1, we summarize a series of commonly used MOFs to compare their molecular building block, lattice, and morphology of the crystals.⁵⁶

Furthermore, MOF particles with different crystal habits can be obtained by stabilizing different exposed facets of the same MOF structure under different experimental conditions. Zeolite imidazolate framework-8 (ZIF-8) is a standard example, which features a sodalite lattice with a monovalent Zn²⁺ node in Td symmetry. A ZIF-8 single crystal can be controlled into three different morphologies, namely rhombic dodecahedron (RD), truncated dodecahedron (TRD), and truncated cube (TC) by applying different synthetic procedures. The RD ZIF-8 exposes the (110) plane, the TRD ZIF-8 exposes both (110) and (111), and the TC ZIF-8 exposes both (110) and (100) planes (Figure 3).^{21,29,43,44} Since different crystal planes have different densities of metal sites and different voids, the interactions between different facets vary widely, resulting in different assembly styles.

When comparing the assembly of MOF particles with other types of particles, the distinctive feature that governs the assembly process is the geometric shape of the building block. Metal nanoparticles, which are typically spherical in shape and relatively small at the tens of nanometer scale, tend to form face-centered cubic or hexagonal structures with the close-packing arrangement. The interparticle interactions between metal nanoparticles, such as electrostatic interactions, hydrophobic-hydrophobic interactions, and DNA hybridization, play an essential role in governing the assembly process.^{57–59} By carefully adjusting the strength and distance of these particle-particle interactions, the final assembled structures of the metal nanoparticles can be significantly impacted.^{60–62} In contrast, non-spherical MOF single crystals possess unique crystal habits that primarily influence their assembly style. The unique geometry and exposed facets of MOF particles give rise to distinct assembly characteristics. For example, ZIF-8 particles with shapes such as RD or cube favor face-to-face stacking mode that can strengthen non-specific interactions between particles.²¹ By evaporating solvent to induce the assembly of ZIF-8 particles, the RD ZIF-8 particles with exposed (110) organized into a close packing arrangement, while the assembly of the TC ZIF-8 particles changed into a simple cubic packing mode due to the stronger face-to-face interactions.^{21,63} In addition, MOF particles can also be easily post-functionalized with surface capping agents, which allows another degree of control over particle arrangement at the macroscale.²⁰ Since long-range ordered assemblies, such as superlattices, are usually compact and closely interacted, they tend to be more stable than disordered assemblies.

Surface modification and interaction

Considering the assembly process involving the spontaneous organization of individual components into more complex structures, interparticle interactions are critical for the assembly of particles, as they determine the strength of the interactions and the properties of the

Table 1. Summary of the building blocks, lattice structures, and morphology of the crystal of commonly used MOFs

MOF	Building Block	Symmetry & Connectivity	Lattice	Crystal Habit	Exposed Facet	EM Image	Reference
MOF-5	Zn ₄ O(COO) ₆ + BDC	<i>T_d</i> , 6	Simple cubic	Cube	(1 0 0)		Li et al. ⁴⁰ , Choi et al. ⁴²
ZIF-8	ZnN ₄ + 2-MIm	<i>T_d</i> , 4	Simple cubic	Rh dodecahedron (RD) Truncated RD Truncated cube	(1 1 0) (1 1 0) & (1 1 1) (1 1 0) & (1 0 0)		Avci et al. ²⁹ , Yanai et al. ⁴³ , Cravillon et al. ⁴⁴
UiO-66	Zr ₆ O ₄ (OH) ₄ (COO) ₁₂ + BDC	<i>O_h</i> , 12	Face-centered cubic	Octahedron	(1 1 1)		Cavka et al. ⁴¹ , Lyu et al. ⁴⁵
NU-1000	Zr ₆ O ₄ (OH) ₈ (H ₂ O) ₄ (COO) ₈ + TBAPy	<i>O_h</i> , 8	Simple hexagonal	Spindle shape	(1 1 0) & (1 0 0)		Mondloch et al. ⁴⁶ , Webber et al. ⁴⁷
PCN-224	Zr ₆ O ₄ (OH) ₁₀ (H ₂ O) ₆ (COO) ₆ + TCPP	<i>O_h</i> , 6	Body-centered cubic	Cube	(1 0 0)		Feng et al. ⁴⁸ , Shi et al. ⁴⁹
MIL-53(Fe)	FeO ₄ (OH) ₂ 1D chain + BDC	<i>P₂₁</i>	Simple triclinic	Spindle shape	(0 0 1) & (1 0 0)		Chen et al. ⁵⁰ , Zheng et al. ⁵¹
MIL-101(Fe)	Fe ₃ O(H ₂ O) ₂ Cl(COO) ₆ + BDC	<i>D_{3h}</i> , 6	Face-centered cubic	Octahedron	(1 1 1)		Celeste et al. ⁵² , Ho et al. ⁵³
HKUST-1	Cu ₂ (H ₂ O) ₂ (COO) ₄ + BTC	<i>D_{4h}</i> , 4	Face-centered cubic	Octahedron	(1 1 1)		Goyal et al. ⁵⁴ , Liu et al. ⁵⁵

The abbreviations used in Table 1. BDC = Terephthalate, 2-MIm = 2-Methylimidazole, TBAPy = 1,3,6,8-tetrakis(p-benzoate)pyrene, TCPP = meso-tetrakis(4-carboxylate-phenyl)porphyrin, BTC = benzene-1,3,5-tricarboxylate, Rh=Rhombic. The scale bars are 10 μm for MOF-5; 5 μm for PCN-224, MIL-53(Fe), and HKUST-1; 1 μm for NU-1000; 500 nm for MIL-101(Fe), ZIF-8; 200 nm for UiO-66. All the SEM images are reproduced with permission from the listed references.

resulting structure. On the surface of a pristine MOF particle, the interparticle forces mainly rely on the open metal sites and exposed ligands. A variety of functional ligands can also be installed on the surface of MOF particles, providing more programmable and precise control of the behavior of the assembled structures (Figure 4). Here, we discuss the surface modifications and interactions of pristine and functionalized MOFs. We further explore the potential of these interactions for the construction of facet-controlled macroscopic MOF structures.

For pristine, unmodified MOF particles, intermolecular forces between exposed metal sites and functional groups on the organic ligands are largely responsible for particle assembly. For instance, the surface of MOF particles typically carries positive charges, which can facilitate electrostatic adsorption between particles through the presence of molecules with a negative charge.⁴³ The organic ligands on the surfaces of MOFs, which contain both donor and acceptor units,⁶⁴ can induce assembly via hydrogen bonds or coordination interactions to the unsaturated metal sites. Moreover, the assembly of unmodified MOF particles can be guided by molecules in the microenvironment, such as solvents and surfactants. These molecules can increase charge or hydrogen bonding interactions, as well as act as connecting links.^{45,65} Additionally, these molecules can also provide attractive depletion interactions between particles due to osmotic pressure.^{21,66} For instance, when

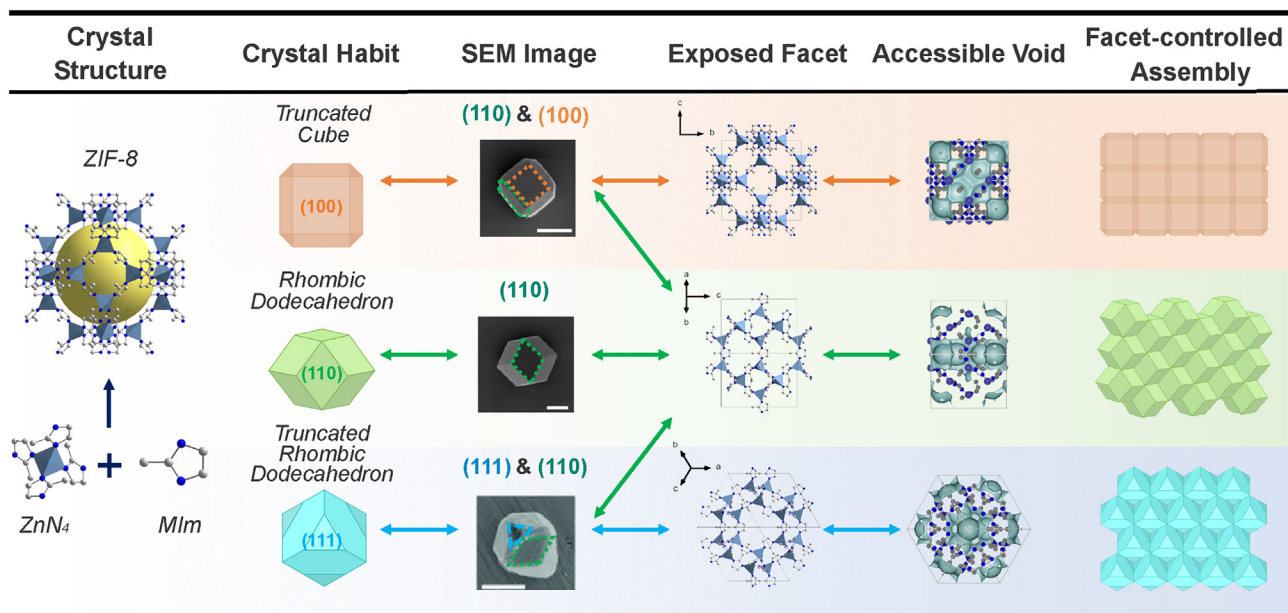


Figure 3. The ZIF-8 particles have three distinct crystal habits

ZIF-8 particles with different shapes expose different facets and voids, resulting in different assembly styles. Scale bars are 500 nm for RD- and TC-ZIF-8, and 1 μm for TRD-ZIF-8. The SEM images presented here are adapted with permission from ref.²⁹ (Copyright 2015, Wiley-VCH) and ref.⁴⁵ (Copyright 2022, The Authors).

the concentration of colloidal particles is high enough, the solvent or surfactant molecules are excluded from the “depletion zone” between the particles, leading to an unbalanced solution. Consequently, adjacent particles will be pushed together to fill the gap in the “depletion zone” between particles due to the osmotic pressure. This process will repeat, ultimately resulting in the assembly of all particles in the solution.

To enhance the programmability and stability of interparticle interactions, as well as to achieve higher-order MOF constructs with greater control over their structures and properties, functional ligands can be incorporated onto the MOF particle surface to facilitate the assembly process.^{20,64} Various functional ligands can be introduced via coordination, host-guest interaction, ligand exchange, covalent modification, etc. For example, the open metal nodes on the MOF surface, also known as the coordinatively unsaturated sites, can be modulated with capping molecules containing carboxyl, sulfonic acids, phosphates, and other coordination motifs.^{67,68} The exposed ligands can also be functionalized using ligand exchange or covalent modification on reactive motifs, such as $-\text{OH}$, $-\text{NH}_2$, and $-\text{CH}=\text{CH}_2$.^{9,69,70} The surface coordination approach on metal sites is relatively straightforward and reversible, while ligand exchange and modification is more stable and resistant to degradation. The incorporated surface agents on the functionalized MOF can then be used to guide the assembly of particles to form more robust extended MOF materials. This enables precise and controllable assembly of MOF particles, allowing for facet, orientation, and spatial control with a high degree of accuracy.

Thermodynamic view of the assembly process

When MOF particles are assembled, it is a thermodynamic process driven by the Gibbs free energy associated with the formation of different assembly modes with different energy states. Ideally, the difference in energy between the MOF particles before and after assembly is the driving force that pulls them together and external energy is required to overcome the energy barriers during the transition between different assembled states.^{71,72} It is notable that for hard particle assembly, the particle organization modes are primarily determined by orientational and positional entropy maximization, with a minor contribution from enthalpy.⁷³ Therefore, in the assembly process of MOF particles with different crystal habits, the interaction is largely determined by entropy, resulting in the entropically more favorable face-to-face mode of assembly, which tends to result in particles being stacked closely.^{72,74,75}

Considering this, we conceptually scheme different MOF particle organizations associated with Gibbs free energy states (Figure 5). The initial state corresponds to the non-assembled state, wherein individual MOF particles are dispersed in solution, leading to a high surface energy attributed to the extensive exposed surface areas. This state is normally thermodynamically unstable and favors aggregation in the bulk solution. As a result, after standing for a period of time, the dispersed particles tend to occupy a local minimum state. The state can be either a metastable state with simple clusters or a kinetically trapped state with relatively disordered MOF particle arrangements.^{71,75} For instance, in the ice-template method using freeze-drying, MOF particles only form a quasi-ordered superstructure due to the high mechanical stress, resulting in a kinetically trapped state.⁶³

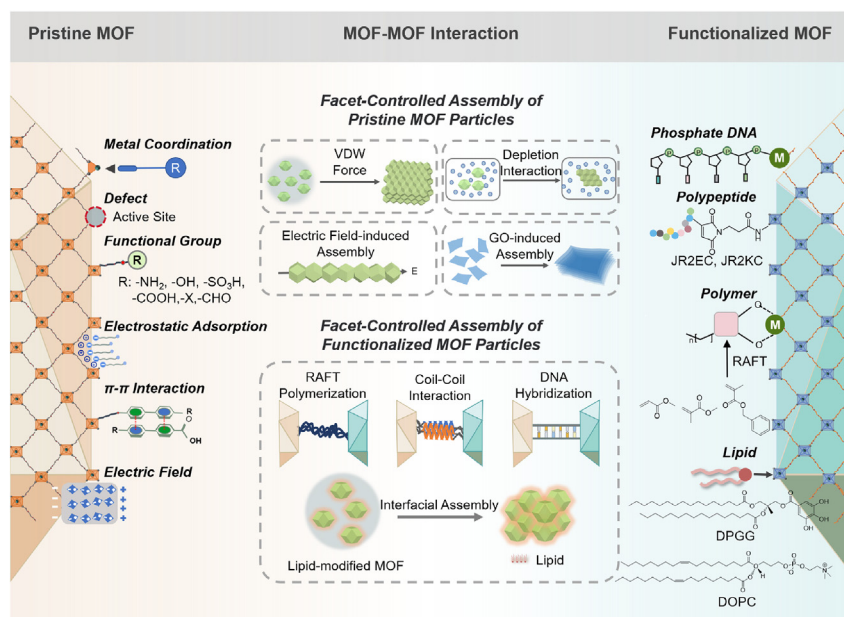


Figure 4. An illustration overview of various surface modifications and interactions that occur on pristine and functionalized MOF particles It also outlines how the facet-controlled assembly is guided by different types of MOF-MOF interactions.

Furthermore, applying an external action that provides enough thermal energy to overcome the thermodynamic barriers, such as adding surfactants and slowly evaporating, or undergoing annealing followed by a slow cooling process, can guide the assembly of MOF particles in the metastable or kinetically trapped state to reach a thermodynamic equilibrium state with a global minimum energy. This thermodynamic equilibrium state leads to compactly organized MOF structures with well-controlled facets and long-range order. These structures are stable and do not require further energy to maintain their form, even in the presence of external effects.^{19,76} In the next section, we will review different methods for generating facet-controlled MOF assemblies.

METHODS TO REALIZE FACET-CONTROLLED ASSEMBLY

Self-assembly of MOF particles can occur in solution or at various interfaces such as gas-liquid, liquid-liquid, and liquid-solid, forming structures including 1D chains, 2D films, and 3D superlattices.^{16,20,76,77} The formation of organized MOF structures depends on adjusting surface interactions and environmental factors such as particle shape, capping agents, applied forces, temperature, and other conditions.^{19,21,43,45} In this section, based upon the types of MOF surface modifications and the ways that particles interact with each other, we have summarized the reported assembly approaches into three categories: spontaneous assembly, external forces-guided assembly, and surface modification-induced assembly, highlighting the forces and particle interactions, methods for facet and orientation control, and the unique properties and potential applications of the resulting MOF materials.

Spontaneous assembly

The most widely used approach is so-called spontaneous assembly, which directly organizes the unmodified MOF particles into high-order structures via nonspecific interactions, such as van der Waals force, hydrogen bonds, charge attraction, π - π stacking, etc.

A key interaction for spontaneous assembly is using depletion force to induce MOF assembly, which typically starts by evaporating solvent molecules or adding large depletion agents. The depletion molecules are more thermodynamically favorable in solution than surrounding the MOF particles, leading to MOF particles coming together under osmotic pressure to form various assembled structures. (Figure 6A).^{66,78,79} Granick and co-workers demonstrated the facet-controlled ordered assembly of ZIF-8 particles through gradual solvent evaporation.⁴³ In the case of ZIF-8 particles with a defined rhombic dodecahedron shape, MOF superstructures were formed through the face-to-face attraction of particles, and the resulting structure was solidified upon the complete removal of solvents (Figure 6B). At high particle concentrations, the particles connect face-to-face and exhibit (111) crystal planes, resulting in a hexagonal arrangement. At low concentrations, weak particle interactions allow substrate-particle interactions to dominate the assembly, resulting in a (110) plane-exposed structure. The aggregates formed are all part of a face-centered cubic structure, demonstrating that RD-ZIF-8 prefers face-centered cubic assembly structures.

However, the MOF structure generated by evaporation-induced assembly is not very stable and difficult to scale-up. Adding depletion agents to induce the depletion process can bring the MOF particles closer together, resulting in a more stable assembled structure. Hu et al. utilized polyvinylpyrrolidone as a depletion agent to produce facet-controlled MOF assembly. This method allowed for the preparation

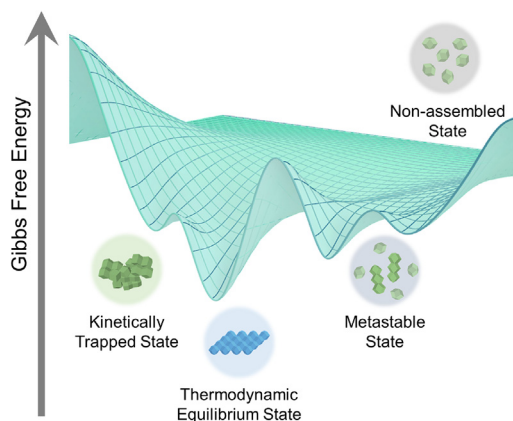


Figure 5. Schematic illustration of the Gibbs free energy diagram representing the relationship between free energy and different MOF particle organization states during assembly

of a single layer of MOF particle assembly with an area of over 10 cm² and the creation of multilayer structures on silicon wafer through repeated transfer processes.⁶⁵ Daniel and colleagues used cetrimonium bromide as a cationic surfactant and depletion agent to produce monodisperse ZIF-8 nanoparticles and self-assembled superstructures through temperature control and solvent evaporation.²¹ The addition of surfactants increased the strength of particle interaction and formed closely packed superlattices. RD-ZIF-8 particles assembled into compact face-centered cubic stacks with (110) stacking and exposed (111) planes, while TC ZIF-8 particles showed a larger face-to-face stacking area, forming oblique simple cubic structures with (100) plane exposure. Wang and colleagues studied the impact of anisotropy in MOF particles and found that MOF particles with different morphologies could form surface-to-surface connections through depletion interactions (Figure 6C).⁴⁵ The assembly of octahedral UiO-66 exposed (111) plane, and truncated hexagonal bipyramidal MIL-96 exposed (101) plane, as shown by SEM images (Figure 6C, right).

In addition to solvent evaporation and depletion agents, there are other ways to achieve facet control in MOF assembly. Yamauchi et al. reported an ice-template method for making 2D MOF superstructures with ordered alignment and assembly without using surfactants or external fields. The MOF particles were ordered by crystallographic alignment and formed quasi-ordered superstructures. By adjusting the concentration of precursor particles, monolayer and bilayer MOF superstructures can be obtained.⁶³ 2D MOF structures can also be assembled with controlled facets and orientations to form multilayered materials.^{76,80} Jiang and colleagues used graphene oxide to assemble copper-1,4-benzenedicarboxylate (Cu-BDC) nanosheets into a laminated arrangement (Figure 6D).⁷⁶ The flexible graphene oxide improved the interlayer interactions and filled the gaps between the rigid MOF nanosheets, resulting in strong and continuous nanosheet membranes with improved gas separation performance compared to non-GO-doped Cu-BDC membranes.

Spontaneous assembly provides a simple way to obtain facet-controlled macroscopic MOF materials with high MOF ratio and preserved properties, without adding non-MOF components. However, the assemblies formed by this method have weak interparticle forces, leading to low stability, and are challenging to make into freestanding materials.

External forces-guided assembly

Another approach to achieving facet-controlled assembly of nanoparticles is through the use of external forces, such as acoustic, electric, and magnetic fields.^{77,81,82} The external electric field can enhance the interparticle electrostatic interactions between MOF surfaces by promoting the dipole-dipole interaction. MOF crystals have different charge distributions and dipole effects on different crystal planes, so applying an electric field can result in more effective facet-controlled connections, leading to the preparation of high-orientation assembly materials (Figure 7A).

Granick and colleagues proposed design rules for electric field-guided polyhedral crystal chain formation. The dipole attraction between crystals drives preferred face-to-face attachment, selective attachment between small surfaces can be achieved by controlling surface area and curvature, and a locked-in chain can be formed even after the removal of the electric field (Figure 7B).⁷⁷ The electric field-induced assembly of three shapes of ZIF-8 particles was studied. The RD-ZIF-8 particles connected well in the direction of the electric field to form a 1D chain structure with (110) crystal planes and good alignment under a low-frequency electric field, which remained stable after removing the electric field. The surface contact projections of particles in the same assembly chain demonstrate the facet and orientation control of the assembly. Jia Min Chin and colleagues used an electric field to assist the assembly of dispersed MOF particles, leading to the formation of highly aligned 3D structures.⁸² The application of the external electric field caused MOF particles with different length-to-diameter ratios to be arranged in an orderly manner along the direction of the electric field and form multilayer and long-range ordered structures (Figure 7C). In the absence of an electric field, MOF particles were disordered, but when the electric field was further applied, they arranged again along the direction of the field. This approach has overcome the long-standing challenge of directional assembly of independent MOF crystals and is applicable not

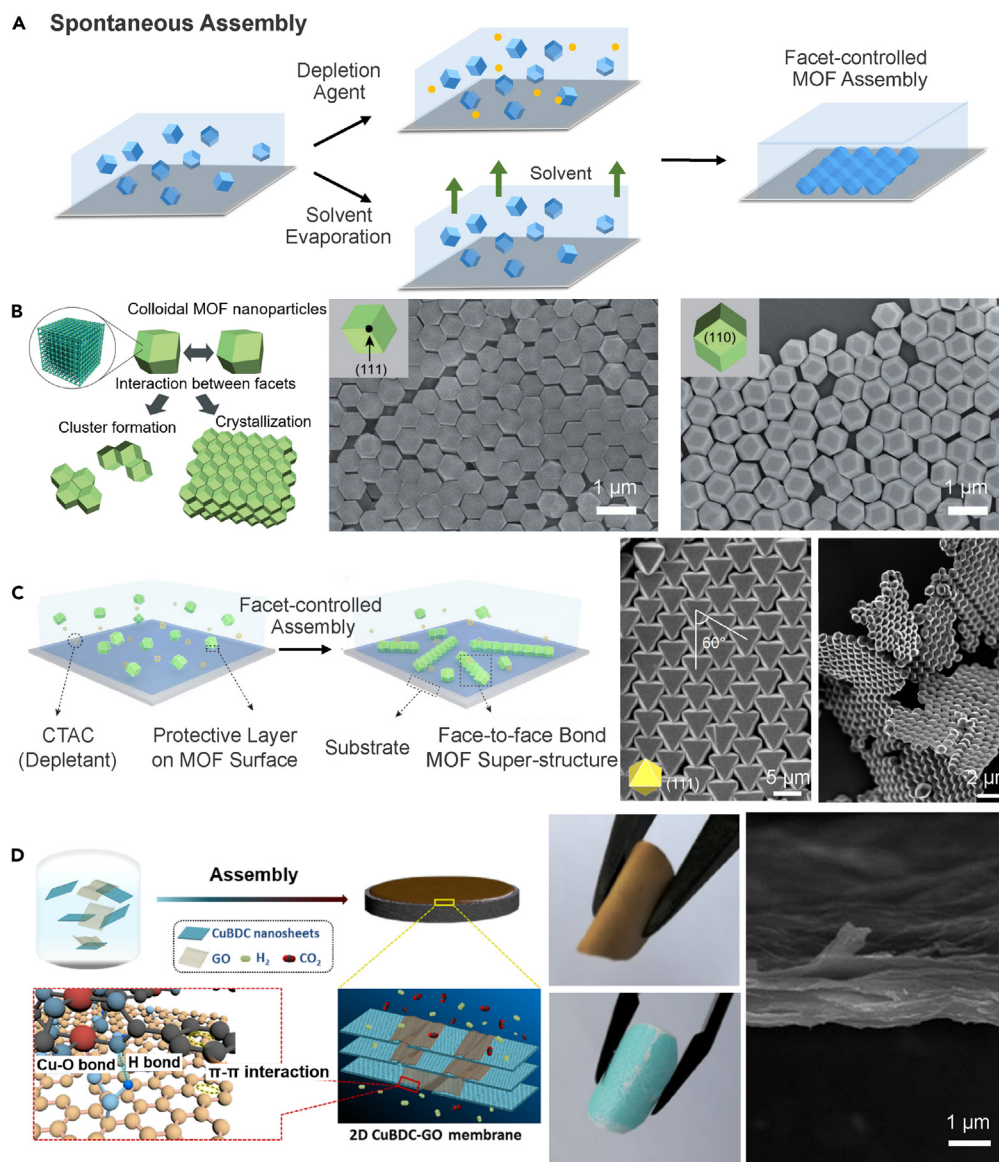


Figure 6. Spontaneous assembly of MOF particles

(A) A schematic illustration depicts MOF particles assembled into facet and orientation-controlled structures through face-to-face stacking via solvent evaporation or the addition of a depletion agent.

(B) Evaporation-induced MOF particle assembly. When assembling MOF particles at high concentrations, the face-to-face interaction between particles is stronger and results in exposure of the (111) crystal plane in the assembly structure. However, at low concentrations, the interaction between particle faces and the substrate dominates, leading to exposure of the (110) plane in the assembly structure. Scale bar = 1 μm . (Reproduced with permission from ref.⁴³, Copyright 2012, Wiley-VCH).

(C) The depletion interaction between MOF particles enhances face-to-face stacking and results in exposure of (111) plane in the assembly structure of UiO-66 and (101) plane in the assembly structure of MIL-96. Left SEM image: scale bar = 5 μm ; Right SEM image: scale bar = 2 μm . (Reproduced with permission from ref.⁴⁵, Copyright 2022, The Authors).

(D) GO-induced assembly of Cu-BDC nanosheets. The graphene oxide-doped film has improved flexibility and strength compared to the undoped film. The uniformity of the assembled film is evident in the cross-section SEM image (right). Scale bar = 1 μm . (Reproduced with permission from ref.⁷⁶, Copyright 2019, American Chemical Society).

only to particles with low L/D ratios but also to particles with high polydispersity, making it an effective strategy for facet-controlled MOF particle assembly. In addition, the use of a magnetic field has also been reported for successful facet-controlled assembly of MOFs. While the magnetic field has also shown the capability to induce directional alignment of MOF particles, further improvement is needed to achieve greater order and control in the assembly process.⁸¹ In addition, other forms of external forces can also serve as potential interventions to

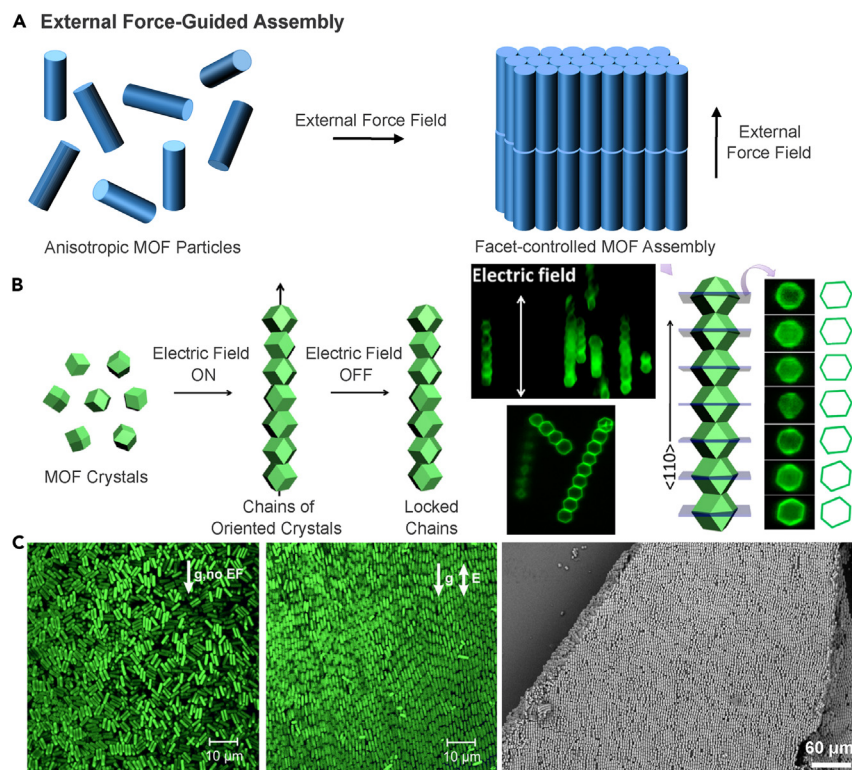


Figure 7. External force-guided assembly of MOF particles

(A) Schematic illustration of MOF particles being orderly assembled along the direction of the applied force field.

(B) The electric field-induced RD-ZIF-8 assembly. After the electric field was applied, ZIF-8 particles formed one-dimensional chains along the direction of the electric field, and this structure was retained even after the electric field was removed. (Reproduced with permission from ref.⁷⁷, Copyright 2012, American Chemical Society).

(C) Without the electric field, the MOF particles were disordered (left, scale bar = 10 μm), but when the electric field was applied, the MOF particles aligned in the direction of the electric field (middle, scale bar = 10 μm), resulting in a long-range ordered assembly structure (right, scale bar = 60 μm). (Reproduced with permission from ref.⁸², Copyright 2021, The Authors).

regulate the assembly process of MOF particles. For instance, acoustic forces have been applied to control the assembly of various particles, including polystyrene particles, cells, and covalent organic nanotubes.^{83,84} By leveraging similar material design principles, acoustic-controlled MOF particle assembly can also be achieved.

Surface modification-induced assembly

The assembly of MOF particles can be hindered by low binding affinity and the resulting materials are often not freestanding. To address these limitations and enhance the applications of MOFs, it is crucial to modify the exposed functional ligands and unsaturated metal sites on MOF particles through post-synthetic modification. Adding surface modification units can increase interaction possibilities between particles, such as covalent bonds, supramolecular interactions, and DNA hybridizations, leading to better programmability and tunability in MOF assembly (Figure 8A).

There have been several studies investigating the modification and assembly of MOFs using polymers. These polymers can form strong supramolecular forces through hydrogen bonding or hydrophobic interactions between chains, allowing for crosslinking of MOF particles. In 2018, Huo et al. used polymethyl methacrylate (PMMA) to create a self-assembled capsule structure of ZIF-8, which improved its selective catalytic properties by encapsulating an enzyme.⁶⁹ Jeffrey Brinker and colleagues have also explored using phenolic lipids to encapsulate and functionalize MOF particles. These modifications maintained the structural integrity and porosity of MOFs, making them useful for various applications, including forming 2D monolayer arrays through evaporation-induced interface assembly.⁸⁷ Cohen and co-workers published a study on the self-assembly of a porous monolayer freestanding membrane using PMMA-modified ZIF-8 MOF particles with improved facet control.¹⁶ PMMA can be grafted onto the surface of MOFs through ligand exchange and polymerization after synthesis, allowing for self-assembly through the supramolecular interactions between polymers (Figure 8B). This method improves the content of MOFs in the assembly, resulting in better utilization of the MOF's properties. The self-assembled monolayer and multilayer structures can be prepared at the liquid-gas interface with different MOFs, extending this method to a wider range of frameworks.⁸⁵ By adjusting the size of MOFs and the length and

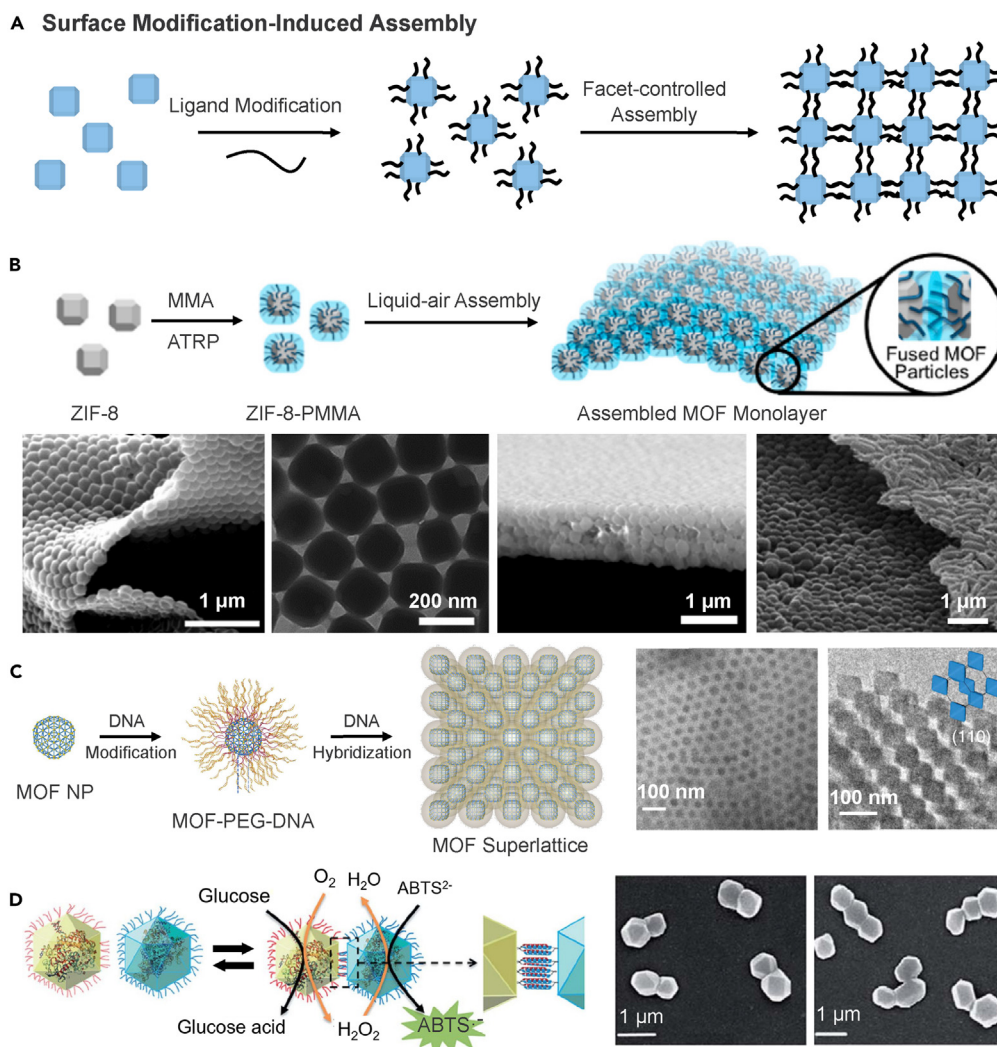


Figure 8. Surface modification-induced assembly of MOF particles

(A) The assembly of MOF particles is directed by the interactions between the surface-modified ligands.

(B) PMMA can be grafted onto the surface of MOF particles through ligand exchange and polymerization reaction after synthesis. The facet-controlled assembly of MOF particles can be achieved through the supramolecular interactions between polymers on the liquid-gas interface. Scale bars from left to right: 1 μm , 200 nm, 1 μm , and 1 μm . (Reproduced with permission from ref.¹⁶, Copyright 2019, American Chemical Society, and ref.⁶⁵, Copyright 2020, The Royal Society of Chemistry).

(C) DNA-mediated programmable assembly of MOF particles into different superlattices. UiO-66 can form body-centered cubic stacking mode and PCN-222 can form hexagonal arrangement mode. Scale bar = 100 nm. (Reproduced with permission from ref.²⁰, Copyright 2020, The Authors).

(D) Polypeptide-induced MOF particle assembly. The dimeric and trimeric MOF assembly structure can be formed by adjusting the peptides modified on the MOF surface. Scale bar = 1 μm . (Reproduced with permission from ref.⁸⁶, Copyright 2019, The Royal Society of Chemistry).

hydrophobicity of grafted polymers, the facet orientation of MOFs in the formed membrane can be controlled, leading to membranes with improved properties.¹⁹

Assembly of MOF particles can be achieved with high specificity and facet control through the surface-modified biomolecules such as DNA and peptides.^{20,86} This method is based on the precise molecular recognition abilities of these biomolecules, which is a contrast to the non-specific interaction between polymers. Mirkin and colleagues modified UiO-66 particles with complementary DNA sequences and created 3D superlattices through DNA base pairing (Figure 8C). The length of the linker DNA affected the structure of the assembly. Longer DNA chains resulted in more spherical particles that tended to form a face-centered cubic or hexagonal lattice. When shorter DNA strands were used, the MOF particles maintained their original morphology and formed a body-centered cubic lattice or quadrilateral lattice.²⁰ Liang and colleagues modified ZIF-8 MOF particles with peptides through ligand exchange and covalent modification, leading to the specific assembly of MOF particles via helical peptide interactions (Figure 8D). By introducing different

polypeptide molecules onto MOF, they were able to form assemblies with two or three MOF particles, facilitating cascade reactions using loaded enzymes.⁸⁶ Through the post-modification of MOFs, more interaction modes and stronger forces can be introduced during assembly, resulting in a more stable structure with better arrangement control. However, excessive modification can weaken the MOF particle anisotropy and block the accessible voids, so the balance between stability, processability, and orientation is important for the construction of functional porous materials.

PERSPECTIVE

In this perspective article, we focus on facet-controlled assembly as a promising route for fabricating MOF crystalline powders into large, orderly, and functional materials. We delve into the key concepts of the MOF assembly process, including the geometry of building blocks, surface functions, and Gibbs free energy landscape. We have reviewed the three main approaches to realize facet-controlled MOF assembly, spontaneous assembly, assembly guided by external forces, and assembly induced by surface modification, which are classified based on the way MOF particles interact with one another.

Despite initial advancements, the development of better synthetic methods and exploration of potential applications for MOF assemblies remain challenging. One major challenge lies in processing individual nanometer or micrometer-scale MOF particles into centimeter-scale, highly ordered materials, such as well-aligned MOF filter membranes. These materials can be utilized in various configurations, such as being supported on substrates, self-supported, or even as freestanding structures. The defining feature of these ordered structures is their well-organized arrangement, which leads to enhanced properties compared to random aggregation. However, most reported methods that can achieve high facet and orientation control typically result in ordered MOF arrangements with only a few tens of micrometers in size, limiting their practical applications, especially in industrial settings. To address this challenge, one potential solution is to explore well-established processing procedures used for other materials, such as quantum dots and photonic crystals, and adapt them for fabricating centimeter-scale, ordered MOF assemblies.^{88,89} By drawing insights from these well-established methods, we can pave the way for more practical applications of MOF materials.

Another challenge in the fabrication of facet-controlled MOF assemblies is finding a balance between crosslinking specificity and the desired properties of the resulting material. When MOF assembly lacks linker molecules, selectivity and stability may be low due to weak particle interactions. Using strong and programmable linkers such as DNA or peptides increase specificity and control, but can hinder MOF properties such as catalytic activity and porosity by blocking pores and covering metal sites. A potential solution is using porous linkers like molecular cages and crown ethers, which have intrinsic porosity, to facilitate particle assembly through reversible and gentle supramolecular interactions.^{90–92}

Finally, the potential applications of facet-controlled MOF assemblies still need to be fully explored. The precise organization of specific facets with metal centers in assembled MOF particles can lead to improved efficiency and selectivity in catalysis. Additionally, the precise control of MOF arrays with uniform open channels can result in the creation of highly selective and efficient membranes with improved mass transfer rates, which can have a wide range of applications, including water purification, biochemical separation, and batteries.

In conclusion, the possibilities of facet-controlled MOF assembly are vast and varied. With the progress in surface modification techniques, the surface properties and interactions of MOF particles can be controlled, resulting in the creation of diverse materials from MOF particles with different sizes, shapes, and properties. These advanced materials have the potential for enhanced adsorption, separation, and catalysis and can be used in fields such as sensing, bioimaging, and biomedical applications.

ACKNOWLEDGMENTS

This work was financially supported by NSFC (21877032), Hunan Provincial Science and Technology Department (2022SK2003, 2022JJ10007), the Science & Technology Innovation Program of Hunan Province (2022RC3046), and Shenzhen Institute of Synthetic Biology Scientific Research Program (DWKF20210005).

DECLARATION OF INTERESTS

All other authors declare they have no competing interests.

REFERENCES

1. Wang, S., McGuirk, C.M., d'Aquino, A., Mason, J.A., and Mirkin, C.A. (2018). Metal–Organic Framework Nanoparticles. *Adv. Mater.* **30**, e1800202.
2. Zhou, H.C.J., and Kitagawa, S. (2014). Metal–Organic Frameworks (MOFs). *Chem. Soc. Rev.* **43**, 5415–5418.
3. Furukawa, H., Cordova, K.E., O’Keeffe, M., and Yaghi, O.M. (2013). The Chemistry and Applications of Metal–Organic Frameworks. *Science* **341**, 1230444.
4. Majewski, M.B., Noh, H., Islamoglu, T., and Farha, O.K. (2018). NanoMOFs: little crystallites for substantial applications. *J. Mater. Chem. A* **6**, 7338–7350.
5. Cui, Y., Li, B., He, H., Zhou, W., Chen, B., and Qian, G. (2016). Metal–Organic Frameworks as Platforms for Functional Materials. *Acc. Chem. Res.* **49**, 483–493.
6. Haase, F., Hirschele, P., Freund, R., Furukawa, S., Ji, Z., and Wuttke, S. (2020). Beyond Frameworks: Structuring Reticular Materials across Nano–Meso–and Bulk Regimes. *Angew. Chem. Int. Ed.* **59**, 22350–22370.
7. Zhang, Y., Feng, X., Li, H., Chen, Y., Zhao, J., Wang, S., Wang, L., and Wang, B. (2015). Photoinduced Postsynthetic Polymerization of a Metal–Organic Framework toward a Flexible Stand-Alone Membrane. *Angew. Chem. Int. Ed.* **54**, 4259–4263.
8. Zhang, C., Wu, B.-H., Ma, M.-Q., Wang, Z., and Xu, Z.-K. (2019). Ultrathin metal/covalent–organic framework membranes towards ultimate separation. *Chem. Soc. Rev.* **48**, 3811–3841.
9. Nagata, S., Kokado, K., and Sada, K. (2015). Metal–organic framework tethering PNIPAM for ON–OFF controlled release in solution. *Chem. Commun.* **51**, 8614–8617.

10. Li, J., Wang, J., Li, Q., Zhang, M., Li, J., Sun, C., Yuan, S., Feng, X., and Wang, B. (2021). Coordination Polymer Glasses with Lava and Healing Ability for High-Performance Gas Sieving. *Angew. Chem. Int. Ed.* **60**, 21304–21309.
11. Turetsky, D., Alzate-Sánchez, D.M., Wasson, M.C., Yang, A., Noh, H., Atilgan, A., Islamoglu, T., Farha, O.K., and Dichtel, W.R. (2022). Hot Press Synthesis of MOF/Textile Composites for Nerve Agent Detoxification. *ACS Mater. Lett.* **4**, 1511–1515.
12. Widmer, R.N., Lampronti, G.I., Anzellini, S., Gaillac, R., Farsang, S., Zhou, C., Belenguer, A.M., Wilson, C.W., Palmer, H., Kleppe, A.K., et al. (2019). Pressure promoted low-temperature melting of metal-organic frameworks. *Nat. Mater.* **18**, 370–376.
13. Makiura, R., Motoyama, S., Umemura, Y., Yamanaka, H., Sakata, O., and Kitagawa, H. (2010). Surface nano-architecture of a metal-organic framework. *Nat. Mater.* **9**, 565–571.
14. Kalaj, M., Denny, M.S., Jr., Bentz, K.C., Palomba, J.M., and Cohen, S.M. (2019). Nylon–MOF Composites through Postsynthetic Polymerization. *Angew. Chem. Int. Ed.* **58**, 2336–2340.
15. Datta, S.J., Mayoral, A., Murthy Srivatsa Bettahalli, N., Bhatt, P.M., Karunakaran, M., Carja, I.D., Fan, D., Graziane M Mileo, P., Semino, R., Maurin, G., et al. (2022). Rational design of mixed-matrix metal-organic framework membranes for molecular separations. *Science* **376**, 1080–1087.
16. Katayama, Y., Kalaj, M., Barcus, K.S., and Cohen, S.M. (2019). Self-Assembly of Metal–Organic Framework (MOF) Nanoparticle Monolayers and Free-Standing Multilayers. *J. Am. Chem. Soc.* **141**, 20000–20003.
17. Deng, K., Luo, Z., Tan, L., and Quan, Z. (2020). Self-assembly of anisotropic nanoparticles into functional superstructures. *Chem. Soc. Rev.* **49**, 6002–6038.
18. Falcaro, P., Okada, K., Hara, T., Ikgaki, K., Tokudome, Y., Thornton, A.W., Hill, A.J., Williams, T., Doonan, C., and Takahashi, M. (2017). Centimetre-scale micropore alignment in oriented polycrystalline metal-organic framework films via heteroepitaxial growth. *Nat. Mater.* **16**, 342–348.
19. Barcus, K., Lin, P.-A., Zhou, Y., Arya, G., and Cohen, S.M. (2022). Influence of Polymer Characteristics on the Self-Assembly of Polymer-Grafted Metal–Organic Framework Particles. *ACS Nano* **16**, 18168–18177.
20. Wang, S., Park, S.S., Buru, C.T., Lin, H., Chen, P.-C., Roth, E.W., Farha, O.K., and Mirkin, C.A. (2020). Colloidal crystal engineering with metal-organic framework nanoparticles and DNA. *Nat. Commun.* **11**, 2495.
21. Avci, C., Imaz, I., Carné-Sánchez, A., Pariente, J.A., Tasios, N., Pérez-Carvajal, J., Alonso, M.I., Blanco, A., Dijkstra, M., López, C., and Maspocho, D. (2017). Self-assembly of polyhedral metal-organic framework particles into three-dimensional ordered superstructures. *Nat. Chem.* **10**, 78–84.
22. Ikgaki, K., Okada, K., Tokudome, Y., Toyao, T., Falcaro, P., Doonan, C.J., and Takahashi, M. (2019). MOF-on-MOF: Oriented Growth of Multiple Layered Thin Films of Metal–Organic Frameworks. *Angew. Chem. Int. Ed.* **58**, 6886–6890.
23. Gu, C., Hosono, N., Zheng, J.-J., Sato, Y., Kusaka, S., Sakaki, S., and Kitagawa, S. (2019). Design and control of gas diffusion process in a nanoporous soft crystal. *Science* **363**, 387–391.
24. Fan, F., Zhang, Z., Zeng, Q., Zhang, L., Zhang, X., Wang, T., and Fu, Y. (2022). Oriented self-assembly of metal-organic frameworks driven by photoinitiated monomer polymerization. *RSC Adv.* **12**, 19406–19411.
25. Okada, K., Mori, K., Fukatsu, A., and Takahashi, M. (2021). Oriented growth of semiconducting TCNQ@Cu₃(BTC)₂ MOF on Cu(OH)₂: crystallographic orientation and pattern formation toward semiconducting thin-film devices. *J. Mater. Chem. A* **9**, 19613–19618.
26. Ma, Z.-Z., Li, Q.-H., Wang, Z., Gu, Z.-G., and Zhang, J. (2022). Electrically regulating nonlinear optical limiting of metal-organic framework film. *Nat. Commun.* **13**, 6347.
27. Bux, H., Feldhoff, A., Cravillon, J., Wiebcke, M., Li, Y.-S., and Caro, J. (2011). Oriented Zeolitic Imidazolate Framework-8 Membrane with Sharp H₂/C₃H₈ Molecular Sieve Separation. *Chem. Mater.* **23**, 2262–2269.
28. Fonseca, J., Meng, L., Imaz, I., and Maspocho, D. (2023). Self-assembly of colloidal metal-organic framework (MOF) particles. *Chem. Soc. Rev.* **52**, 2528–2543.
29. Avci, C., Ariñez-Soriano, J., Carné-Sánchez, A., Guillerm, V., Carbonell, C., Imaz, I., and Maspocho, D. (2015). Post-Synthetic Anisotropic Wet-Chemical Etching of Colloidal Sodalite ZIF Crystals. *Angew. Chem. Int. Ed.* **54**, 14417–14421.
30. Whitesides, G.M., and Boncheva, M. (2002). Beyond molecules: Self-assembly of mesoscopic and macroscopic components. *Proc. Natl. Acad. Sci.* **99**, 4769–4774.
31. Grzybowski, B.A., and Campbell, C.J. (2004). Complexity and dynamic self-assembly. *Chem. Eng. Sci.* **59**, 1667–1676.
32. Grzybowski, B.A., Wilmer, C.E., Kim, J., Browne, K.P., and Bishop, K.J.M. (2009). Self-assembly: from crystals to cells. *Soft Matter* **5**, 1110–1128.
33. Elghanian, R., Storhoff, J.J., Mucic, R.C., Letsinger, R.L., and Mirkin, C.A. (1997). Selective Colorimetric Detection of Polynucleotides Based on the Distance-Dependent Optical Properties of Gold Nanoparticles. *Science* **277**, 1078–1081.
34. Alivisatos, A.P., Johnsson, K.P., Peng, X., Wilson, T.E., Loweth, C.J., Bruchez, M.P., and Schultz, P.G. (1996). Organization of 'nanocrystal molecules' using DNA. *Nature* **382**, 609–611.
35. Brodin, J.D., Auyeung, E., and Mirkin, C.A. (2015). DNA-mediated engineering of multicomponent enzyme crystals. *Proc. Natl. Acad. Sci.* **112**, 4564–4569.
36. Park, S.Y., Lytton-Jean, A.K.R., Lee, B., Weigand, S., Schatz, G.C., and Mirkin, C.A. (2008). DNA-programmable nanoparticle crystallization. *Nature* **451**, 553–556.
37. Wang, Y., Wang, Y., Zheng, X., Ducrot, É., Lee, M.-G., Yi, G.-R., Weck, M., and Pine, D.J. (2015). Synthetic Strategies Toward DNA-Coated Colloids that Crystallize. *J. Am. Chem. Soc.* **137**, 10760–10766.
38. Gartner, Z.J., and Bertozzi, C.R. (2009). Programmed assembly of 3-dimensional microtissues with defined cellular connectivity. *Proc. Natl. Acad. Sci.* **106**, 4606–4610.
39. Urban, J.J., Talapin, D.V., Shevchenko, E.V., and Murray, C.B. (2006). Self-Assembly of PbTe Quantum Dots into Nanocrystal Superlattices and Glassy Films. *J. Am. Chem. Soc.* **128**, 3248–3255.
40. Li, H., Eddaoudi, M., O'Keeffe, M., and Yaghi, O.M. (1999). Design and synthesis of an exceptionally stable and highly porous metal-organic framework. *Nature* **402**, 276–279.
41. Cavka, J.H., Jakobsen, S., Olsbye, U., Guillou, N., Lamberti, C., Bordiga, S., and Lillerud, K.P. (2008). A New Zirconium Inorganic Building Brick Forming Metal Organic Frameworks with Exceptional Stability. *J. Am. Chem. Soc.* **130**, 13850–13851.
42. Choi, J.-S., Son, W.-J., Kim, J., and Ahn, W.-S. (2008). Metal-organic framework MOF-5 prepared by microwave heating: Factors to be considered. *Microporous Mesoporous Mater.* **116**, 727–731.
43. Yanai, N., and Granick, S. (2012). Directional Self-Assembly of a Colloidal Metal–Organic Framework. *Angew. Chem. Int. Ed.* **51**, 5638–5641.
44. Cravillon, J., Schröder, C.A., Bux, H., Rothkirch, A., Caro, J., and Wiebcke, M. (2012). Formate modulated solvothermal synthesis of ZIF-8 investigated using time-resolved *in situ* X-ray diffraction and scanning electron microscopy. *CrystEngComm* **14**, 492–498.
45. Lyu, D., Xu, W., Payong, J.E.L., Zhang, T., and Wang, Y. (2022). Low-dimensional assemblies of metal-organic framework particles and mutually coordinated anisotropy. *Nat. Commun.* **13**, 3980.
46. Mondloch, J.E., Bury, W., Fairen-Jimenez, D., Kwon, S., DeMarco, E.J., Weston, M.H., Sarjeant, A.A., Nguyen, S.T., Stair, P.C., Snurr, R.Q., et al. (2013). Vapor-Phase Metalation by Atomic Layer Deposition in a Metal–Organic Framework. *J. Am. Chem. Soc.* **135**, 10294–10297.
47. Webber, T.E., Liu, W.-G., Desai, S.P., Lu, C.C., Truhlar, D.G., and Penn, R.L. (2017). Role of a Modulator in the Synthesis of Phase-Pure NU-1000. *ACS Appl. Mater. Interfaces* **9**, 39342–39346.
48. Feng, D., Chung, W.-C., Wei, Z., Gu, Z.-Y., Jiang, H.-L., Chen, Y.-P., Darensbourg, D.J., and Zhou, H.-C. (2013). Construction of Ultrastable Porphyrin Zr Metal–Organic Frameworks through Linker Elimination. *J. Am. Chem. Soc.* **135**, 17105–17110.
49. Shi, L., Yang, L., Zhang, H., Chang, K., Zhao, G., Kako, T., and Ye, J. (2018). Implantation of Iron(III) in porphyrinic metal organic frameworks for highly improved photocatalytic performance. *Appl. Catal., B* **224**, 60–68.
50. Chen, H., Yuan, X., Jiang, L., Wang, H., Yu, H., and Wang, X. (2022). Intramolecular modulation of iron-based metal organic framework with energy level adjusting for efficient photocatalytic activity. *Appl. Catal., B* **302**, 120823.
51. Zheng, X., Qi, S., Cao, Y., Shen, L., Au, C., and Jiang, L. (2021). Morphology evolution of acetic acid-modulated MIL-53(Fe) for efficient selective oxidation of H₂S. *Chinese J. Catal.* **42**, 279–287.
52. Celeste, A., Paolone, A., Itié, J.P., Borondics, F., Joseph, B., Grad, O., Blanita, G., Zlotea, C., and Capitani, F. (2020). Mesoporous Metal–Organic Framework MIL-101 at High Pressure. *J. Am. Chem. Soc.* **142**, 15012–15019.
53. Ho, C.-K., Li, C.-Y.V., Gao, L., Chan, K.-Y., Chen, J., Tang, J., Olorunoyi, J.F., Liao, C., and Zhao, T. (2021). Protonated Emeraldine Polyaniline Threaded MIL-101 as a Conductive High Surface Area Nanoporous Electrode. *ACS Energy Lett.* **6**, 3769–3779.
54. Goyal, P., Paruthi, A., Menon, D., Behara, R., Jaiswal, A., Keerthy, V., Kumar, A., Krishnan, V., and Misra, S.K. (2022). Fe doped bimetallic

- HKUST-1 MOF with enhanced water stability for trapping Pb(II) with high adsorption capacity. *Chem. Eng. J.* **430**, 133088.
55. Liu, B., Li, Y., Oh, S.C., Fang, Y., and Xi, H. (2016). Fabrication of a hierarchically structured HKUST-1 by a mixed-ligand approach. *RSC Adv.* **6**, 61006–61012.
56. Bai, Y., Dou, Y., Xie, L.-H., Rutledge, W., Li, J.-R., and Zhou, H.-C. (2016). Zr-based metal-organic frameworks: design, synthesis, structure, and applications. *Chem. Soc. Rev.* **45**, 2327–2367.
57. Kalsin, A.M., Fialkowski, M., Paszewski, M., Smoukov, S.K., Bishop, K.J.M., and Grzybowski, B.A. (2006). Electrostatic Self-Assembly of Binary Nanoparticle Crystals with a Diamond-Like Lattice. *Science* **312**, 420–424.
58. Macfarlane, R.J., Lee, B., Jones, M.R., Harris, N., Schatz, G.C., and Mirkin, C.A. (2011). Nanoparticle Superlattice Engineering with DNA. *Science* **334**, 204–208.
59. Nicolas-Boluda, A., Yang, Z., Dobryden, I., Carn, F., Winckelmans, N., Péchoux, C., Bonville, P., Bals, S., Claesson, P.M., Gazeau, F., and Pileni, M.P. (2020). Intracellular Fate of Hydrophobic Nanocrystal Self-Assemblies in Tumor Cells. *Adv. Funct. Mater.* **30**, 2004274.
60. Jones, M.R., Seaman, N.C., and Mirkin, C.A. (2015). Programmable materials and the nature of the DNA bond. *Science* **347**, 1260901.
61. McMillan, J.R., Hayes, O.G., Winegar, P.H., and Mirkin, C.A. (2019). Protein Materials Engineering with DNA. *Acc. Chem. Res.* **52**, 1939–1948.
62. Laramy, C.R., O'Brien, M.N., and Mirkin, C.A. (2019). Crystal engineering with DNA. *Nat. Rev. Mater.* **4**, 201–224.
63. Song, Y., Song, X., Wang, X., Bai, J., Cheng, F., Lin, C., Wang, X., Zhang, H., Sun, J., Zhao, T., et al. (2022). Two-Dimensional Metal-Organic Framework Superstructures from Ice-Templated Self-Assembly. *J. Am. Chem. Soc.* **144**, 17457–17467.
64. Rimoldi, M., Howarth, A.J., DeStefano, M.R., Lin, L., Goswami, S., Li, P., Hupp, J.T., and Farha, O.K. (2017). Catalytic Zirconium/Hafnium-Based Metal-Organic Frameworks. *ACS Catal.* **7**, 997–1014.
65. Lu, G., Cui, C., Zhang, W., Liu, Y., and Huo, F. (2013). Synthesis and Self-Assembly of Monodispersed Metal-Organic Framework Microcrystals. *Chem. Asian J.* **8**, 69–72.
66. Young, K.L., Personick, M.L., Engel, M., Damasceno, P.F., Barnaby, S.N., Bleher, R., Li, T., Glotzer, S.C., Lee, B., and Mirkin, C.A. (2013). A Directional Entropic Force Approach to Assemble Anisotropic Nanoparticles into Superlattices. *Angew. Chem. Int. Ed.* **52**, 13980–13984.
67. Koutsianos, A., Kazimierska, E., Barron, A.R., Taddei, M., and Andreoli, E. (2019). A new approach to enhancing the CO₂ capture performance of defective UiO-66 via post-synthetic defect exchange. *Dalton Trans.* **48**, 3349–3359.
68. Wang, S., McGuirk, C.M., Ross, M.B., Wang, S., Chen, P., Xing, H., Liu, Y., and Mirkin, C.A. (2017). General and Direct Method for Preparing Oligonucleotide-Functionalized Metal-Organic Framework Nanoparticles. *J. Am. Chem. Soc.* **139**, 9827–9830.
69. Xu, Z., Xiao, G., Li, H., Shen, Y., Zhang, J., Pan, T., Chen, X., Zheng, B., Wu, J., Li, S., et al. (2018). Compartmentalization within Self-Assembled Metal-Organic Framework Nanoparticles for Tandem Reactions. *Adv. Funct. Mater.* **28**, 1802479.
70. Liu, C., Li, T., and Rosi, N.L. (2012). Strain-Promoted “Click” Modification of a Mesoporous Metal-Organic Framework. *J. Am. Chem. Soc.* **134**, 18886–18888.
71. Sorrenti, A., Leira-Iglesias, J., Markvoort, A.J., de Greef, T.F.A., and Hermans, T.M. (2017). Non-equilibrium supramolecular polymerization. *Chem. Soc. Rev.* **46**, 5476–5490.
72. Rao, A., Roy, S., Jain, V., and Pillai, P.P. (2023). Nanoparticle Self-Assembly: From Design Principles to Complex Matter to Functional Materials. *ACS Appl. Mater. Interfaces* **15**, 25248–25274.
73. Damasceno, P.F., Engel, M., and Glotzer, S.C. (2012). Predictive Self-Assembly of Polyhedra into Complex Structures. *Science* **337**, 453–457.
74. Whitesides, G.M., and Grzybowski, B. (2002). Self-Assembly at All Scales. *Science* **295**, 2418–2421.
75. van Rossum, S.A.P., Tena-Solsona, M., van Esch, J.H., Eelkema, R., and Boekhoven, J. (2017). Dissipative out-of-equilibrium assembly of man-made supramolecular materials. *Chem. Soc. Rev.* **46**, 5519–5535.
76. Yang, F., Wu, M., Wang, Y., Ashtiani, S., and Jiang, H. (2019). A GO-Induced Assembly Strategy To Repair MOF Nanosheet-Based Membrane for Efficient H₂/CO₂ Separation. *ACS Appl. Mater. Interfaces* **11**, 990–997.
77. Yanai, N., Sindoro, M., Yan, J., and Granick, S. (2013). Electric Field-Induced Assembly of Monodisperse Polyhedral Metal-Organic Framework Crystals. *J. Am. Chem. Soc.* **135**, 34–37.
78. Pang, J., Xiong, S., Jaeckel, F., Sun, Z., Dunphy, D., and Brinker, C.J. (2008). Free-Standing, Patternable Nanoparticle/Polymer Monolayer Arrays Formed by Evaporation Induced Self-Assembly at a Fluid Interface. *J. Am. Chem. Soc.* **130**, 3284–3285.
79. Henzie, J., Grünwald, M., Widmer-Cooper, A., Geissler, P.L., and Yang, P. (2011). Self-assembly of uniform polyhedral silver nanocrystals into densest packings and exotic superlattices. *Nat. Mater.* **11**, 131–137.
80. Jose, N.A., Varghese, J.J., Mushrif, S.H., Zeng, H.C., and Lapkin, A.A. (2021). Assembly of Two-Dimensional Metal Organic Framework Superstructures via Solvent-Mediated Oriented Attachment. *J. Phys. Chem. C* **125**, 22837–22847.
81. Cheng, F., Marshall, E.S., Young, A.J., Robinson, P.J., Bouillard, J.-S.G., Adawi, A.M., Vermeulen, N.A., Farha, O.K., Reithofer, M.R., and Chin, J.M. (2017). Magnetic Control of MOF Crystal Orientation and Alignment. *Chem. Eur J.* **23**, 15578–15582.
82. Allahyarli, K., Reithofer, M.R., Cheng, F., Young, A.J., Kiss, E., Tan, T.T.Y., Prado-Roller, A., and Chin, J.M. (2022). Metal-Organic Framework superstructures with long-ranged orientational order via E-field assisted liquid crystal assembly. *J. Colloid Interface Sci.* **610**, 1027–1034.
83. Yang, S., Tian, Z., Wang, Z., Rufo, J., Li, P., Mai, J., Xia, J., Bachman, H., Huang, P.-H., Wu, M., et al. (2022). Harmonic acoustics for dynamic and selective particle manipulation. *Nat. Mater.* **21**, 540–546.
84. Koner, K., Karak, S., Kandambeth, S., Karak, S., Thomas, N., Leanza, L., Perego, C., Pesce, L., Capelli, R., Moun, M., et al. (2022). Porous covalent organic nanotubes and their assembly in loops and toroids. *Nat. Chem.* **14**, 507–514.
85. Barcus, K., and Cohen, S.M. (2020). Free-standing metal-organic framework (MOF) monolayers by self-assembly of polymer-grafted nanoparticles. *Chem. Sci.* **11**, 8433–8437.
86. Liang, J., Mazur, F., Tang, C., Ning, X., Chandrawati, R., and Liang, K. (2019). Peptide-induced super-assembly of biocatalytic metal-organic frameworks for programmed enzyme cascades. *Chem. Sci.* **10**, 7852–7858.
87. Zhu, W., Xiang, G., Shang, J., Guo, J., Motevalli, B., Durfee, P., Agola, J.O., Coker, E.N., and Brinker, C.J. (2018). Versatile Surface Functionalization of Metal-Organic Frameworks through Direct Metal Coordination with a Phenolic Lipid Enables Diverse Applications. *Adv. Funct. Mater.* **28**, 1705274.
88. Cai, Z., Li, Z., Ravaine, S., He, M., Song, Y., Yin, Y., Zheng, H., Teng, J., and Zhang, A. (2021). From colloidal particles to photonic crystals: advances in self-assembly and their emerging applications. *Chem. Soc. Rev.* **50**, 5898–5951.
89. Pietryga, J.M., Park, Y.-S., Lim, J., Fidler, A.F., Bae, W.K., Brovelli, S., and Klimov, V.I. (2016). Spectroscopic and Device Aspects of Nanocrystal Quantum Dots. *Chem. Rev.* **116**, 10513–10622.
90. Liang, Y., Li, E., Wang, K., Guan, Z.-J., He, H.-H., Zhang, L., Zhou, H.-C., Huang, F., and Fang, Y. (2022). Organo-macrocyclic-containing hierarchical metal-organic frameworks and cages: design, structures, and applications. *Chem. Soc. Rev.* **51**, 8378–8405.
91. Montà-González, G., Sancenón, F., Martínez-Máñez, R., and Martí-Centelles, V. (2022). Purely Covalent Molecular Cages and Containers for Guest Encapsulation. *Chem. Rev.* **122**, 13636–13708.
92. Yang, X., Zhang, Q., Liu, Y., Nian, M., Xie, M., Xie, S., Yang, Q., Wang, S., Wei, H., Duan, J., et al. (2023). Metal-Organic Framework Nanoparticles with Universal Dispersibility through Crown Ether Surface Coordination for Phase-Transfer Catalysis and Separation Membranes. *Angew. Chem. Int. Ed.* **62**, e202303280.